15th Australasian Wind Engineering Society Workshop
Sydney, Australia
23-24 February 2012

Urban Physics: effects of wind on comfort, energy, health and driving rain

J. Carmeliet[1,2], P. Moonen[1,2], T. Defraeye[3], V. Dorer[2] and B. Blocken[4]

[1]Chair of Building Physics
ETH Zürich 8093, Switzerland

[2]Laboratory of Building Science and Technology
Empa, Dübendorf 8600, Switzerland

[3]CVCBT/MeBioS, Department of Biosystems,
Katholieke Universiteit Leuven 3001 Belgium

[4]Building Physics and Systems
Technical Universiteit Eindhoven 5600, The Netherlands

Introduction

The global trend towards urbanization explains the growing interest in the study of the modification of the urban climate and its impact on energy use of buildings. Also urban comfort, health and durability, referring respectively to pedestrian wind/thermal comfort, pollutant dispersion and driving rain are of interest. Urban Physics is a well-established discipline, incorporating relevant branches of physics, environmental chemistry, aerodynamics, meteorology and statistics. Therefore, Urban Physics is well positioned to provide key-contributions to the existing urban problems and challenges. Wind interaction with the urban morphology plays a determining role in the urban microclimate and building (energy) performance. The present paper addresses the role of wind in the study of wind comfort, energy, pollutant dispersion and wind-driven rain. Case studies illustrate the current challenges and the relevant contributions of wind research to urban physics.

Urban wind comfort

High-rise buildings can introduce high wind speed at pedestrian level, which can lead to uncomfortable or even dangerous conditions. The high wind speed conditions at pedestrian level are caused by the fact that high-rise buildings deviate wind at higher elevations towards pedestrian level. The wind-flow pattern around a building is schematically indicated in Figure 1. The approaching wind (1) is partly guided over the building (3), partly around the vertical edges (4), but the largest part is deviated to the ground-level, where a standing vortex develops (5-6) that subsequently wraps around the corners (8) and joins the overall flow around the building at ground level (9). The typical problem areas where high wind speed occurs are the standing vortex and the corner streams. Further upstream, a stagnation region with low wind speed is present (7). Downstream of the building, complex and strongly transient wind-velocity patterns develop, but these are generally associated with lower wind speed values and are of less concern (10-16). Based on an extensive review of the literature, Blocken and Carmeliet (2004a) identified three other typical problem situations, which are indicated in Figure 2. In all three cases, the increased wind speed is caused by so-called pressure short-circuiting, i.e. the connection between high-pressure and low-pressure areas. Figure 2a shows a passage through a building (gap or through-passage), which can lead to very strong amplifications of wind speed, up to a factor 2.5 – 3 compared to free-field conditions. Figure 2b shows a passage between two buildings. Wind speed in the passage is increased due to the two corner streams from both buildings that merge together in the passage. Amplification factors up to 2 can be obtained this way. Figure 2c finally shows a passage between two shifted parallel buildings. In this case, a rather large area of increased wind speed can occur between the buildings, with amplification values up to 2.

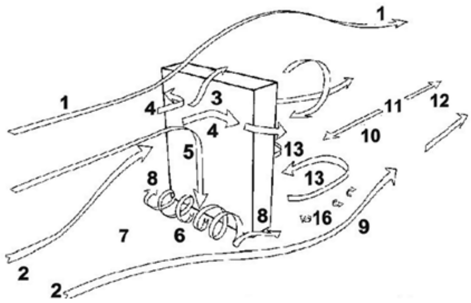

Figure 1: Schematic representation of wind flow pattern around a high-rise building (from Beranek and van Koten 1979).

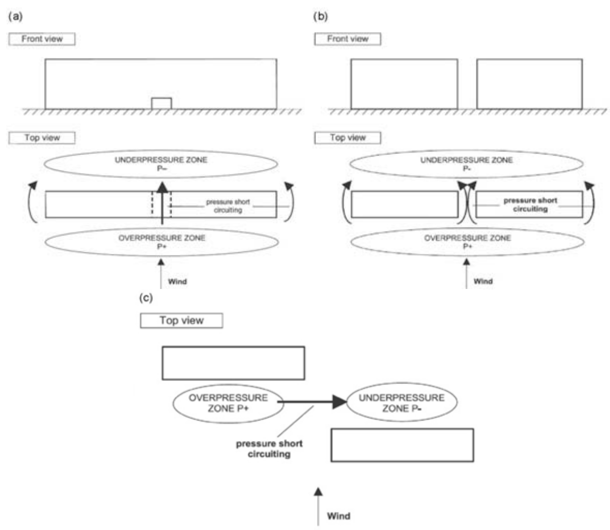

Figure 2: Schematic representation of three situations in which increased wind speed can occur due to pressure-short circuiting: (a) passage through a building; (b) passage between two parallel buildings; (c) passage between two parallel shifted buildings (Blocken and Carmeliet 2004a).

Pedestrian-level wind conditions around buildings and in urban areas can be analysed by on-site measurements, by wind tunnel measurements or by CFD. Wind tunnel studies of pedestrian-level wind conditions are focused on determining the mean wind speed and turbulence intensity at pedestrian height (full scale height z = 1.75 or 2 m). Wind tunnel tests are generally point measurements with Laser Doppler Anemometry (LDA) or Hot Wire Anemometry (HWA). One of the main advantages of CFD in pedestrian-level wind comfort studies is providing whole-flow field data. In spite of its deficiencies, steady RANS modelling with the k-ε model or with other turbulence models has become the most popular approach for pedestrian-level wind studies. Two main categories of studies can be distinguished: (1) fundamental studies, which are typically conducted for simple, generic building configurations to obtain insight in the flow behaviour, for parametric studies and for CFD validation, and (2) applied studies, which provide knowledge of the wind environmental conditions in specific and often much more complex case studies.

Assessment of wind comfort however involves a more extensive methodology in which statistical meteorological data is combined with aerodynamic information and with a comfort criterion. The aerodynamic information is needed to transform the statistical meteorological data from the weather station to the location of interest at the building site, after which it is combined with a comfort criterion to evaluate local wind comfort. The aerodynamic information usually consists of two parts: the terrain related contribution and the design related contribution. The terrain related contribution represents the change in wind statistics from the meteorological site to a reference location near the building site (see Figure 3: transformation from potential wind speed U_{pot} to reference wind speed U_{ref}). The design related contribution represents the change in wind statistics due to the local urban design, i.e. the building configurations (U_{ref} to local wind speed U). Different transformation procedures exist to determine the terrain related contribution; they often employ a simplified model of the atmospheric boundary layer such as the logarithmic mean wind speed profile. The design related contribution (i.e. the wind flow conditions around the buildings at the building site) can be obtained by wind tunnel modelling or by CFD.

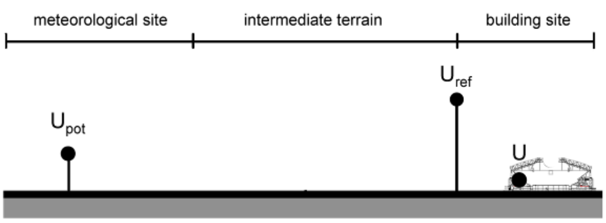

Figure 3: Schematic representation of the wind speed at the meteorological station (Upot), the reference wind speed at the building site (Uref) and the wind speed at the location of interest (U).

Although the use of CFD for the study of pedestrian wind conditions in complex urban configurations is still an issue of debate, it has been employed on a few occasions in the past as part of wind comfort assessment studies (e.g. Richards et al. 2002, Hirsch et al. 2002, Blocken et al. 2004a, Blocken and Carmeliet 2008a, Blocken and Persoon 2009). The use of CFD in such studies is receiving strong support from several international initiatives that specifically focus on the establishment of guidelines for such simulations (Franke et al. 2004, Franke et al. 2007, Yoshie et al. 2007, Tominaga et al. 2008) and from review papers summarizing past achievements and future challenges (Stathopoulos 2002, Blocken and Carmeliet 2004a, 2004b, Franke et al. 2004, Mochida and Lun 2008, Blocken et al. 2011).

Case study

The "Amsterdam ArenA" (Figure 4) is a large multifunctional stadium located in the urban area of south-east Amsterdam. The new urban master plan of the site aims to erect several new high-rise buildings in the stadium vicinity. The current situation is indicated by the grey buildings in Figure 4. The newly planned buildings are indicated in white. The addition of these new buildings raises questions about the future wind comfort at the streets and squares surrounding the stadium. To assess wind comfort in the current situation and in the new situation, an extensive study was performed. This study included on-site wind speed measurements, CFD simulations, validation of the CFD simulations with the measurements and application of the Dutch wind nuisance standard. The CFD simulations were performed with 3D steady RANS and the realizable k-ε model, on a high-resolution grid that was constructed using the body-fitted grid generation technique by van Hooff and Blocken (2010). These simulations were successfully validated based on the wind speed measurements. For the details of the study, the reader is referred to (Blocken and Persoon 2009). Figure 5 shows the main results of the study. Figure 5a and b display contours of the mean wind-velocity ratio $U/U_{ref,60}$ for wind direction 240°. U is the local wind speed at 1.75 m height and $U_{ref,60}$ is the reference free-field wind speed at 60 m height, which is used in the Dutch Standard. Figure 5a shows the present situation, and Figure 5b the situation with newly planned buildings. The addition of the new high-rise tower building with height 150 m clearly yield a strong increase in velocity ratio at the west side of the stadium. When these data, for 12 different wind directions, are combined with the wind statistics, the transformation model and the wind comfort criteria, Figure 5c-d are obtained. They show the exceedance probability of the 5 m/s discomfort threshold. Also here, the negative impact of the new high-rise tower is clear. Finally, these probabilities are converted into quality classes (Figure 5e-f). The main conclusion of the study is that the addition of the high-rise tower has the largest impact. In the present situation, the quality class A at the west side of the stadium refers to a good wind climate for sitting, strolling and walking. However, in the new situation, this area is partly converted to quality class B or C, where C is considered a bad wind climate for sitting, a moderate wind climate for strolling and a sufficiently good wind climate for walking.

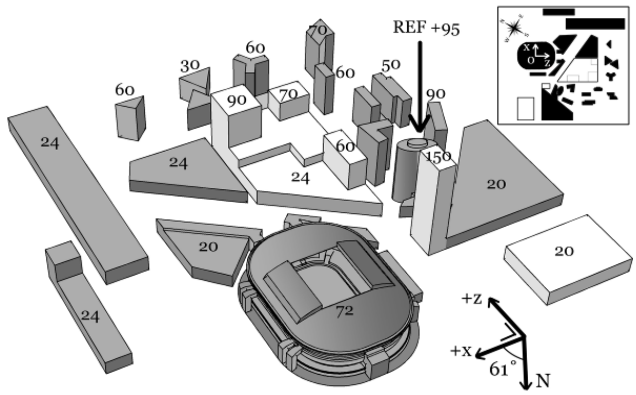

Figure 4: Amsterdam ArenA football stadium and surrounding buildings in a 300 m radius around the stadium. Blocks in grey: current situation; blocks in white: newly planned buildings. The reference measurement position (ABN-Amro tower) and the height of each building are indicated (Blocken and Persoon 2009).

Urban energy demand

As the relative fraction of the urban population is expected to grow up to almost 70% by 2050, the energy consumption in cities is likely to follow that trend. During the next decades, urban planners and stakeholders will have to face major issues in term of energy, traffic and resource flows. Their main concern will certainly be to find adequate ways of planning sustainable energy generation, distribution and storage, but also to increase energy efficiency and reduce demand of non-renewable energies.

Minimizing the energy demand of buildings in urban areas has a great energy-saving potential (Santamouris 2001).

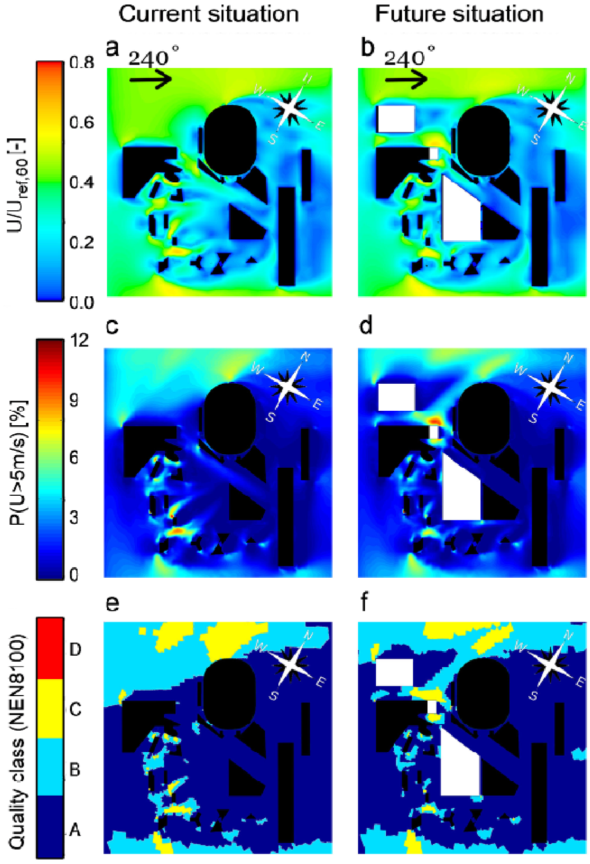

Figure 5: (a-b) Amplification factor $U/U_{ref,60}$; (c-d) exceedance probability P; and (e-f) quality class. All values are taken in a horizontal plane at 2 m above ground-level. Left: current situation; right: situation with newly planned buildings (Blocken and Persoon 2009).

Most building energy simulation codes used today consider buildings as isolated objects, and largely ignore most types of interaction with the environment, except perhaps shadowing. However, urban heat island effects at meso- and microscale as well interactions with the surrounding buildings at local scale do have an important effect on the energy demand of a building in an urban area (Rasheed 2009). As compared to an isolated building, a building in an urban area experiences (i) increased maximum air temperatures due to urban heat island effect; (ii) lower wind speeds due to a wind-sheltering effect; (iii) reduced energy losses during the night due to reduced sky view factors; (iv) altered solar heat gains due to shadowing and reflections; (v) a modified radiation balance due to the interaction with neighbouring buildings. All these effects have an significant impact on the energy demand of buildings (Kolokotroni et al. 2006) since it affects the conductive heat transport through the building envelope, as well as the energy exchange by means of ventilation (Ghiaus 2006), and the modified potential to employ passive cooling (Geros 2005) and renewable energy resources.

There is a wide span of spatial and temporal scales which are relevant when studying the interaction between individual buildings or building clusters and the urban microclimate. The largest scale is probably the regional scale, which captures phenomena such as the heat island effect. At the other end of the spectrum, there is the scale of the individual building and its technical installation. A successful modelling approach to study the energy demand of an individual building or a cluster of buildings in an urban context needs to cover all scales.

At the scale of the individual buildings detailed models exist, such as TRNSYS, IDA-ICE, EnergyPlus or ESP-r. These have to be supplied with suitable boundary conditions, which represent the urban microclimate. Several options exist: (i) heat island effects can be included by means of modified meteorological data, or from meso-scale meteorological models; (ii) radiation trapping and shadowing effects can be accounted for by values found in standards, simple geometrical relationships, or by explicitly modelling the local neighbourhood by means of a radiation model; (iii) convective heat transfer can be based on norm values, measured data or can be derived from CFD simulations. The most complex simulations combine building energy simulation tools with meso-scale meteorological models, radiation models and CFD. Combined or integrated urban microclimate modelling and building energy simulation was mainly advanced in Japan (Ooka 2007, Chen et al. 2009, He et al. 2009).

At urban level there exist many tools for the design and planning of energy supply and distribution systems, based on assumed or measured annual or seasonal building energy demand figures. However, in order to consider interactions between energy demand and the urban microclimate, more complex tools are needed, as e.g. the CitySim simulation platform (Robinson et al. 2011). The tool consists of a collection of building physics models such as radiation, thermal, energy conversion and HVAC that were designed to conduct hourly simulations at the urban scale. Each building is modelled explicitly to allow calculations of interactions between buildings and group of buildings through energy and matter exchanges.

Prototypes of software platforms for the total analysis of urban climate were described by (Murakami 2004, Tanimoto et al. 2004, Mochida and Lun 2008). They are mostly based on meso-scale meteorological models and employ urban canopy parameterisations to account for lower-scale phenomena such as the impact of urban surfaces (roofs, walls, streets) on wind speed, temperature, turbulent kinetic energy, shadowing, and radiation trapping. Most studies mostly consider the buildings as stand-alone buildings, and do not take into account their (e.g. radiative) interaction with the local neighbourhood. Allegrini et al. (2011) showed that this practise may lead to huge differences in the predicted energy demand. They considered a stand-alone office building and a building surrounded by street canyons. In the latter, (i) measured field data were used to include the urban heat island effect; (ii) heat transfer coefficients determined by CFD were employed to account for the convective heat transfer; and (iii) radiative exchange was explicitly modelled taking into account the real geometry. In the considered case, the modified radiation balance was the main reason for the different energy demand. The other two aspects – heat island effect and convective energy losses – only had a secondary effect.

Anthropogenic heat fluxes such as heat released by air-conditioning facilities can have an important impact on urban environment and are to be accounted for in more complete studies of urban canopy climate such as urban heat island processes (Krpo 2009) and in building cooling/heating energy demand analysis.

In summary, to evaluate the building energy demand in detail in a specific urban environment, a multiscale approach has to be adopted. The building's radiation balance depends to a large extent on the urban setting and thus has to be considered in detail. Shading effects not only affect the radiation balance, but also influence demand for artificial lighting and therefore the energy consumption (Strømann-Andersen and Sattrup 2011). Also convective losses and the urban heat island effect play an important role in the energy demand. Additionally, effects such as evaporative cooling from wet surfaces and evapotranspiration from urban greenery have an impact on the urban microclimate (Saneinejad et al. 2011). Integrated approaches in urban design are becoming increasingly apparent (Santamouris 2006).

Urban pollutant dispersion

Air pollution in the urban atmosphere can have an adverse impact on the climate, on the environment and on human health (Brunekreef and Holgate, 2002). The transport sector is responsible for a significant share of these emissions in the urban environment (O'Mahony et al., 2000). Other sources of emissions are industrial applications, domestic heating and cooling systems in residential buildings and the accidental and/or deliberate release of toxic agents into the atmosphere. After being emitted, the pollutants are dispersed (i.e. advected and diffused) over a wide range of horizontal length scales. The dispersion process is to a large extent affected by the characteristics of the flow field, which in turn is dominated by the complex interplay between meteorological conditions and urban morphology. During transport, chemically active pollutants might react with other substances and form reaction products. Traffic-induced emissions such as NO_x and VOC are for instance the main precursors of tropospheric ozone. Furthermore, the concentration of airborne compounds is also affected by deposition processes. Distinction is made between so-called wet and dry deposition processing, depending on whether or not coagulation of pollutants with water droplets takes place. From the preceding concise overview, it is clear that accurately predicting outdoor air quality is extremely complicated. In view of its importance, numerous studies have been performed in the past decades to arrive at a better understanding of pollutant emission, dispersion and deposition processes. Insight herein can help to develop measures to improve air quality, to reduce climate change, and to minimize the negative impact on the environment and human health.

A comprehensive review of air pollution aerodynamics was recently compiled by Meroney (2004), addressing the wide range of methods that exist for predicting pollutant dispersion, ranging from field tests and wind tunnel simulations to semi-empirical methods and numerical simulations with Computational Fluid Dynamics (CFD). Numerical simulation with CFD offers some advantages compared to other methods: it is often said to be less expensive than field and wind tunnel tests and it provides results of the flow features at every point in space simultaneously. However, CFD requires specific care in order for the results to be reliable. Therefore, CFD simulations should be performed in accordance with the existing best practise guidelines (Franke et al. 2007, 2011; Blocken et al. 2007b; Tominaga et al., 2008) and should be validated based on high-accuracy experimental data (CODASC, 2008; CEDVAL; CEDVAL-LES).

Several studies have compared the performance of RANS and LES approaches for pollutant dispersion in idealized urban geometries like street canyons (Walton and Cheng, 2002; Salim et al., 2011a,b; Tominaga and Stathopoulos, 2011) and arrays of buildings (Chang 2006; Dejoan et al. 2010). Other efforts have compared RANS and LES for isolated buildings (Tominaga and Stathopoulos, 2010; Yoshie et al., 2011), courtyards (Moonen et al. 2011), and in real urban environments (Hanna et al., 2006; Gousseau et al., 2011). Overall, LES appears to be more accurate than RANS in predicting the mean concentration field because it captures the unsteady concentration fluctuations. Moreover, this approach provides the statistics of the concentration field which can be of prime importance for practical applications. The predictive quality of RANS-type models highly depends on the turbulent Schmidt number (Riddle et al., 2004; Tang et al., 2005; Meroney et al. 1999; Banks et al. 2003; Blocken et al. 2008b). LES models allow updating the Schmidt number dynamically.

Many studies have pointed out that urban building arrangements, in particular the width-to-height ratios of streets, their orientation and the presence of intersections, are critical parameters governing pollution dispersion at street level. Soulhac et al. (2009) conducted numerical simulations of flow and dispersion in an urban intersection and compared the simulation results with wind tunnel measurements. They found that the average concentration along a finite-length street is significantly lower from that observed in an infinitely long street. Furthermore, they observed that the amount of vertical mixing remains limited, which leads to higher concentration levels at street level. Research towards passive measures of pollutant dispersion control has been conducted. The influence of avenue-like tree planting on pollutant dispersion was investigated by means of wind tunnel measurements (Gromke et al. 2008). It was shown that tree planting reduces the air change rate of an urban street canyon, and leads to increased concentrations on the leeward wall and slightly decreased concentrations at the windward wall. The effect is more pronounced for tree crowns with a smaller porosity.

Case study

As an example, the case study by Gousseau et al. (2011) for near-field gas dispersion in downtown Montreal is briefly reported. The aim of the work by Gousseau et al. (2011) was to provide a near-field dispersion study around a building group in downtown Montreal on a high-resolution grid. The focus is both on the prediction of pollutant concentrations in the surrounding streets (for pedestrian outdoor air quality) and on the prediction of concentrations on building surfaces (for ventilation system inlets placement and indoor air quality). The CFD simulations were compared with detailed wind-tunnel experiments performed earlier by Stathopoulos et al. (2004), in which sulfur-hexafluoride (SF6) tracer gas was released from a stack on the roof of a three-storey building and concentrations were measured at several locations on this roof and on the facade of a neighbouring high-rise building (Figure 6a). Note that earlier CFD studies for the same case included none or only one of the neighbouring buildings (Blocken et al. 2008b; Lateb et al. 2010), while in this study by Gousseau et al. (2011), surrounding buildings are included up to a distance of 300 m, in line with the best practice guidelines by Franke et al. (2007, 2011) and Tominaga et al. (2008). A high-resolution grid with minimum cell sizes down to a few centimetres (full-scale) was generated using the procedure by van Hooff and Blocken (2010) (Figure 6b). The grids were obtained based on detailed grid-sensitivity analysis. Both RANS and LES simulations are performed. The RANS simulations were performed with the standard k-ε model (SKE) and the LES simulations with the dynamic Smagorinsky SGS model. For more details about the computational parameters and settings, including boundary conditions, the reader is referred to the original publication. Figure 7 shows the contours of the non-dimensional concentration coefficient K on the building and street surfaces, for south-west wind, about with RANS SKE and LES. For the RANS case shown in this figure, a turbulent Schmidt number Sct = 0.7 has been used. Finally, The comparison between the simulation results and the wind tunnel measurements confirms the sensitivity of the RANS results to the turbulent Schmidt number and the overall good performance by LES.

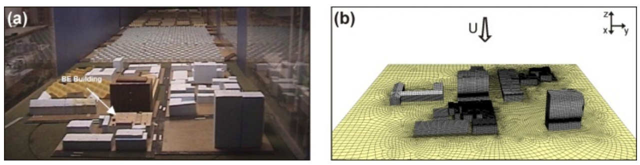

Figure 6: Case study of near-field gas dispersion in downtown Montreal: (a) wind-tunnel model and (b) corresponding computational grid on the building and ground surfaces (Gousseau et al. 2011).

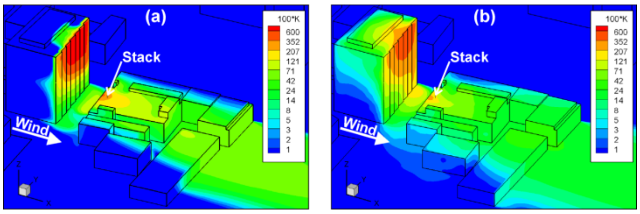

Figure 7: Contours of 100*K on building surfaces and surrounding streets for south-west wind obtained with (a) RANS SKE - Sct = 0.7 and (b) LES (Gousseau et al. 2011).

Urban wind-driven rain

Wind-driven rain (WDR) is one of the most important moisture sources affecting the hygrothermal performance and durability of building facades (Blocken and Carmeliet 2004c). Consequences of its destructive properties can take many forms. Moisture accumulation in porous materials can lead to rain water penetration (Day et al. 1955, Marsh 1977), frost damage (Price 1975, Stupart 1989, Maurenbrecher and Suter 1993, Franke et al. 1998), moisture induced salt migration (Price 1975, Franke et al. 1998), discolouration by efflorescence (Eldridge 1976, Franke et al. 1998), structural cracking due to thermal and moisture gradients (Franke et al. 1998), to mention just a few. WDR impact and runoff is also responsible for the appearance of surface soiling patterns on facades that have become characteristic for so many of our buildings (White 1967, Camuffo et al. 1982, Davidson et al. 2000). Assessing the intensity of WDR on building facades is complex, because it is influenced by a wide range of parameters: building geometry, environment topography, position on the building facade, wind speed, wind direction, turbulence intensity, rainfall intensity and raindrop-size distribution.

Three categories of methods exist for the assessment of WDR on building facades: (1) measurements, (2) semi-empirical methods and (3) numerical methods based on Computational Fluid Dynamics (CFD). An extensive literature review of each of these categories was provided by Blocken and Carmeliet (2004c). Given the drawbacks associated with measurements and with semi-empirical methods, researchers realized that further achievements were to be found by employing numerical methods. In the past fifteen years, the introduction of CFD in the area has provided a new impulse in WDR research.

Choi (1991, 1993, 1994, 1997) developed and applied a steady-state simulation technique for WDR, in which the wind-flow field is modelled using the Reynolds-Averaged Navier-Stokes (RANS) equations with a turbulence model to provide closure. The raindrop trajectories are determined by solving the equation of motion of raindrops of different sizes in the wind-flow pattern. This technique has been universally adopted by the WDR research community. In 2002, Blocken and Carmeliet (2002) extended Choi's steady-state simulation technique into the time domain, allowing WDR simulations for real-life transient rain events. The first study of this type was made by Blocken and Carmeliet (2002) for a low-rise test building. Later, the same authors performed more detailed validation studies for the same building (2006, 2007a). In 2004, the extended WDR simulation method by Blocken and Carmeliet was also used by Tang and Davidson (2004) to study the WDR distribution on the high-rise Cathedral of Learning in Pittsburgh. Later validation studies were performed by Briggen et al. (2009). The steady-state CFD technique for WDR was later also used by Persoon et al. (2008) and van Hooff et al. (2011) to study WDR impingement on the stands of football stadia.

The numerical model for the simulation of WDR on buildings, developed by Choi (1991, 1993, 1994a,b) and extended by Blocken and Carmeliet (2002), consists of the five steps outlined as follows: (1) The steady-state wind-flow pattern around the building is calculated using a CFD code. (2) Raindrop trajectories are obtained by injecting raindrops of different sizes in the calculated wind-flow pattern and by solving their equations of motion. (3) The specific catch ratio is determined based on the configuration of the calculated raindrop trajectories. (4) The catch ratio is calculated from the specific catch ratio and from the raindrop-size distribution. (5) From the data in the previous step, catch-ratio charts are constructed for different zones (positions) at the building facade. The experimental data record of reference wind speed, wind direction and horizontal rainfall intensity for a given rain event is combined with the appropriate catch-ratio charts to determine the corresponding spatial and temporal distribution of WDR on the building facade.

This model is referred to as the "Eulerian-Lagrangian" model for WDR, because the Eulerian approach is adopted for wind-flow field, while the Lagrangian approach is used for the rain phase. Recently, Huang and Li (2011) employed an "Eulerian-Eulerian" model for WDR, in which also the rain phase is treated as a continuum, and they successfully validated this model based on the WDR measurements on the VLIET building by Blocken and Carmeliet (2005).

Case study

Hunting Lodge "St. Hubertus" is a monumental building situated in the National Park "De Hoge Veluwe" (Figure 8a). Especially the south-west facade of the building shows severe deterioration caused by WDR and subsequent phenomena such as rain penetration, mould growth, frost damage, salt crystallization and efflorescence, and cracking due to hygrothermal gradients (Figure 8b-e).

Figure 8: (a) Hunting Lodge St. Hubertus and moisture damage at the tower due to wind-driven rain: (b) salt efflorescence; (c) cracking/blistering due to salt crystallisation; (d) rain penetration and discolouration; (e) cracking at inside surface (Briggen et al. 2009).

To analyse the causes for these problems and to evaluate the effectiveness of remedial measures, Building Envelope Heat-Air-Moisture (BE-HAM) simulations are generally conducted. However, these BE-HAM simulations require the spatial and temporal distribution of WDR on the facade as a boundary condition. Therefore, both field measurements and CFD simulations of wind around the building and WDR impinging on the building south-west facade were performed by Briggen et al.

(2009). The field measurements include measurements of wind speed and wind direction, horizontal rainfall intensity (i.e. the rainfall intensity falling on the ground in unobstructed conditions), and WDR intensity on the facade. The WDR measurements were made at 8 positions and by WDR gauges that were designed following the guidelines by Blocken and Carmeliet (2006c). The WDR measurements at the few discrete positions do not give enough information to obtain a complete picture of the spatial distribution of WDR on the south-west facade of the tower. Therefore, they are supplemented by the CFD simulations. First, the WDR measurements were used to validate the CFD simulations, after which the CFD simulations were used to provide the additional WDR intensity information at positions where no WDR measurements were made. Note that for selecting the rain events for CFD validation, the guidelines by (Blocken and Carmeliet 2005) were followed, which are important to limit the measurement errors and in order not to compromise the validation effort. Figure 13a shows the computational grid of the monumental building, in which the detailed geometry of the south-west building facade was reproduced. The CFD simulations were made with steady RANS and the realizable k-ε model and with the Lagrangian approach for WDR. Figure 9b compares measured and simulated catch ratios at the south-west facade at the end of a rain event, during which the wind direction was perpendicular to this south-west facade. The catch ratio is the ratio between the sum of WDR and the sum of horizontal rainfall during this rain event. Given the complexity of the building and of WDR in general, the agreement at the top part of the facade is considered quite good. However, at the bottom of the facade, a large deviation is obtained between simulations and measurements. As discussed by Briggen et al. (2009), this deviation is attributed due to the absence of turbulent dispersion in the Lagrangian raindrop model. This absence will lead to less accurate results at the lower part of high-rise buildings. Future RANS WDR simulations for high-rise buildings should therefore either include turbulent dispersion, or they should employ LES, in which the turbulent dispersion of raindrops can be explicitly resolved.

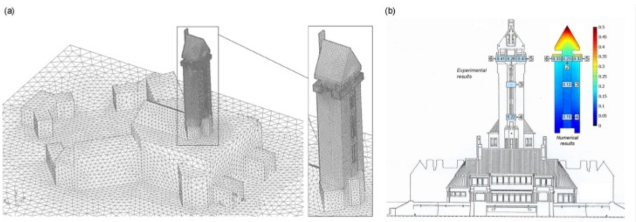

Figure 9: (a) Computational grid (2’110’012 cells). (b) Spatial distribution of the catch ratio at the end of a rain event. The experimental results at the locations of the wind-driven rain gauges are shown on the left, the numerical results are shown on the right (Briggen et al. 2009).

References

Allegrini J, Dorer V, Carmeliet J (2011) Influence on the urban microclimate on the energy demand of buildings. In: Cisbat11 conference, 14-16 Sep. 2011, Lausanne, Switzerland

Banks D, Meroney RN, Petersen RL, Carter JJ (2003) Evaluation of FLUENT for predicting concentrations on buildings. In: A&WMA Conference, San Diego, CA, Paper # 70223

Beranek WJ, Van Koten H (1979) Beperken van windhinder om gebouwen, deel 1, Stichting Bouwresearch no. 65, Kluwer Technische Boeken BV, Deventer (in Dutch)

Blocken B, Carmeliet J (2002) Spatial and temporal distribution of driving rain on a low-rise building. Wind and Structures 5: 441-462

Blocken B, Roels S, Carmeliet J (2004a) Modification of pedestrian wind comfort in the Silvertop Tower passages by an automatic control system, J. of Wind Eng. and Industrial Aerodynamics 92: 849-873

Blocken B, Carmeliet J (2004b) Pedestrian wind environment around buildings: Literature review and practical examples, J. of Thermal Envelope and Building Science 28:107-159

Blocken B, Carmeliet J (2004c) A review of wind-driven rain research in building science, Journal of Wind Engineering and Industrial Aerodynamics 92:1079-1130

Blocken B, Carmeliet J (2005) High-resolution wind-driven rain measurements on a low-rise building – experimental data for model development and model validation. Journal of Wind Engineering and Industrial Aerodynamics 93: 905-928

Blocken B, Carmeliet J (2006) The influence of the wind-blocking effect by a building on its wind-driven rain exposure, Journal of Wind Engineering and Industrial Aerodynamics 94: 101-127

Blocken B, Carmeliet J (2007a) Validation of CFD simulations of wind-driven rain on a low-rise building façade, Building and Environment 42: 2530-2548

Blocken B, Stathopoulos T, Carmeliet J (2007b) CFD simulation of the atmospheric boundary layer: wall function problems. Atmospheric Environment 41: 238-252

Blocken B, Carmeliet J (2008a) Pedestrian wind conditions at outdoor platforms in a high-rise apartment building: generic sub-configuration validation, wind comfort assessment and uncertainty issues, Wind and Structures 11: 51-70.

Blocken B, Stathopoulos T, Saathoff P, Wang X (2008b) Numerical evaluation of pollutant dispersion in the built environment: Comparisons between models and experiments, Journal of Wind Engineering and Industrial Aerodynamics 96: 1817-1831

Blocken B, Persoon J (2009) Pedestrian wind comfort around a large football stadium in an urban environment: CFD simulation, validation and application of the new Dutch wind nuisance standard. J. of Wind Eng. and Industrial Aerodynamics 97: 255-270

Blocken B, Stathopoulos T, Carmeliet J, Hensen JLM (2011) Application of CFD in building performance simulation for the outdoor environment: an overview, Journal of Building Performance Simulation 4: 157-184

Briggen PM, Blocken B, Schellen HL (2009) Wind-driven rain on the facade of a monumental tower: Numerical simulation, full-scale validation and sensitivity analysis, Building and Environment 44: 1675-1690

Brunekreef B, Holgate ST (2002) Air pollution and health. The lancet 360: 1233-1242

Camuffo D, Del Monte M, Sabbioni C, Vittori O (1982) Wetting, deterioration and visual features of stone surfaces in an urban area. Atmospheric Environment 16: 2253–2259

CEDVAL - Compilation of Experimental Data for Validation of Microscale Dispersion Models. Internet Database. Hamburg University, Germany. www.mi.uni-hamburg.de/Introducti.433.0.html

CEDVAL-LES - Compilation of Experimental Data for Validation of Microscale Dispersion LES-Models. Internet Database. Hamburg University, Germany. www.mi.uni-hamburg.de/CEDVAL-LES-V.6332.0.html

Chang CH (2006) Computational fluid dynamics simulation of concentration distributions from a point source in the urban street canyons. J. of Aerospace Eng. 19: 80-86

Chen Q (2009)Ventilation performance prediction for buildings: A method overview and recent applications. Building and Environment 44: 848-858.

Choi ECC (1991) Numerical simulation of wind-driven rain falling onto a 2-D building. In: Asia Pacific Conference on Computational Mechanics, Hong Kong; p. 1721-1728

Choi ECC (1993) Simulation of wind-driven rain around a building, Journal of Wind Engineering and Industrial Aerodynamics 46-47: 721-729

Choi ECC (1994a) Determination of wind-driven rain intensity on building faces, Journal of Wind Engineering and Industrial Aerodynamics 51: 55-69

Choi ECC (1994b) Parameters affecting the intensity of wind-driven rain on the front face of a building, Journal of Wind Engineering and Industrial Aerodynamics 53: 1-17

Choi ECC (1997) Numerical modelling of gust effect on wind-driven rain, Journal of Wind Engineering and Industrial Aerodynamics 72: 107-116

CODASC (2008) Concentration Data of Street Canyons. Internet Database. Karlsruhe Institute of Technology KIT, Germany. www.codasc.de.

Davidson CI, Tang W, Finger S, Etyemezian V, Striegel MF, Sherwood SI (2000) Soiling patterns on a tall limestone building: changes over 60 years, Environmental Science and Technology 34: 560–565

Day AG, Lacy RE, Skeen JW (1955) Rain penetration through walls, A summary of the investigations made at the UK Building Research Station from 1925 to 1955. Building Research Station Note. No. C.364, unpublished.

Dejoan A, Santiago JL, Martilli A, Martin F, Pinelli A (2010) Comparison between Reynolds-Averaged Navier-Stokes computations for the MUST field experiment. Part II: Effects of incident wind angle deviation on the mean flow and plume dispersion, Boundary-Layer Meteorology 135: 133-150

Eldridge HJ (1976) Common defects in buildings, Her Majesty’s Stationary Office, 486 p

Franke L, Schumann I, van Hees R, van der Klugt L, Naldini S, Binda L, Baronio G, Van Balen K, Mateus J (1998) Damage atlas: classification and analyses of damage patterns found in brick masonry, European Commission Research Report No 8, vol. 2, Fraunhofer IRB Verlag

Franke J, Hirsch C, Jensen AG, Krüs HW, Schatzmann M, Westbury PS, Miles SD, Wisse JA, Wright NG (2004) Recommendations on the use of CFD in wind engineering. In: van Beeck JPAJ. (Ed.). Proceedings of the International Conference on Urban Wind Engineering and Building Aerodynamics. COST Action C14, Impact of Wind and Storm on City Life Built Environment. Von Karman Institute, Sint-Genesius-Rode, Belgium, 5–7 May

Franke J, Hellsten A, Schlünzen H, Carissimo B Eds (2007) Best practice guideline for the CFD simulation of flows in the urban environment. COST Action 732: Quality Assurance and Improvement of Microscale Meteorological Models, Hamburg, Germany.

Franke J, Hellsten A, Schlünzen H, Carissimo B (2011) The COST 732 Best Practice Guideline for CFD simulation of flows in the urban environment: a summary, International Journal of Environment and Pollution 44: 419-42

Geros V, Santamouris M, Karatasou S, Tsangrassoulis A, Papanikolaou N (2005) On the cooling potential of night ventilation techniques in the urban environment,. Energy and Buildings 37: 243-257

Ghiaus C, Allard F, Santamouris M, Georgakis C, Nicol F (2006) Urban environment influence on natural ventilation potential, Building and Environment 41: 395-406

Gousseau P, Blocken B, Stathopoulos T, van Heijst GJF (2011) CFD simulation of near-field pollutant dispersion on a high-resolution grid: a case study by LES and RANS for a building group in downtown Montrea,. Atmospheric Environment 45: 428-438

Gromke C, Buccolieri R, Di Sabatino S, Ruck (2008) Dispersion study in a street canyon with tree planting by means of wind tunnel and numerical investigations - evaluation of CFD data with experimental data, Atmospheric Environment 42: 8640-8650

Hanna SR, Brown MJ, Camelli FE, Chan ST, Coirier WJ, Hansen OR, Huber AH, Kim S, Reynolds RM (20069 Detailed simulations of atmospheric flow and dispersion in downtown Manhattan – An application of five computational fluid dynamics models, Bulletin of the American Meteorological Society 87: 1713-1726

He J, Hoyano A, Asawa T (2009) A numerical simulation tool for predicting the impact of outdoor thermal environment on building energy performance, Applied Energy 86: 1596-1605

Hirsch C, Bouffioux V, Wilquem F (2002) CFD simulation of the impact of new buildings on wind comfort in an urban area. In: Workshop Proceedings, Cost Action C14, Impact of Wind and Storm on City Life and Built Environment, Nantes, France.

Huang SH, Li QS (2010) Numerical simulations of wind-driven rain on building envelopes based on Eulerian multiphase model, Journal of Wind Engineering and Industrial Aerodynamics 98: 843-857

Kolokotroni M, Giannitsaris I, Watkins R (2006) The effect of the London Urban Heat Island on building summer cooling demand and night ventilation strategies, Solar Energy: 383-392

Krpo A (2009) Development and application of a numerical simulation system to evaluate the impact of anthropogenic heat fluxes on urban boundary layer climate. PhD thesis, Swiss Federal Institute of Technology Lausanne, 4428

Lateb M, Masson C, Stathopoulos T, Bédard C (20109 Numerical simulation of pollutant dispersion around a building complex, Building and Environment 45: 1788-1798

Marsh P (1977) Air and rain penetration of buildings, The Construction Press Ltd., Lancaster, England, 174 p

Maurenbrecher AHP, Suter GT (1993) Frost damage to clay brick in a loadbearing masonry building, Canadian Journal of Civil Engineering 20: 247–253

Meroney RN, Leitl BM, Rafailidis S, Schatzmann M (1999) Wind tunnel and numerical modelling of flow and dispersion about several building shapes, Journal of Wind Engineering and Industrial Aerodynamics 81: 333–345

Meroney RN (2004) Wind tunnel and numerical simulation of pollution dispersion: a hybrid approach. Working paper, Croucher Advanced Study Insitute on Wind Tunnel Modeling, Hong Kong University of Science and Technology, 6–10 December, 2004, p. 60.

Mochida A, Hataya N, Iwata T, Tabata Y, Yoshino H, Watanabe H (2006) CFD analyses on outdoor thermal environment and air pollutant diffusion in street canyons under the influences of moving automobiles. In: Proceedings of the Sixth International Conference on Urban Climate (ICUC6), Goteborg, Sweden.

Mochida A, Lun IYF (2008) Prediction of wind environment and thermal comfort at pedestrian level in urban area, J. of Wind Eng. and Industrial Aerodynamics 96: 1498-1527

Moonen P, Dorer V, Carmeliet J (2011) Evaluation of the ventilation potential of courtyards and urban street canyons using RANS and LES, Journal of Wind Engineering & Industrial Aerodynamics 99(4): 414-423

Murakami S (2004) Indoor/outdoor climate design by CFD based on the Software Platform. Intern. J. of Heat and Fluid Flow 25: 849–863

O'Mahony M, Gill LW, Broderick BM, English L, Ahern A (2000) Scope of transport impacts on the environment. Environmental Research Technological Development and Innovation (ERTDI) Programme 2000-2006 Report Series No. 9.

Ooka R (2007) Recent development of assessment tools for urban climate and heat-island investigation especially based on experiences in Japan, Intern. J. of Climatology 27: 1919–1930

Persoon J, van Hooff T, Blocken B, Carmeliet J, de Wit MH (2008) Impact of roof geometry on rain shelter in football stadia, Journal of Wind Engineering and Industrial Aerodynamics 96: 1274-1293

Price CA (1975) The decay and preservation of natural building stone, Chemistry in Britain 11: 350–353

Rasheed A (2009) Multiscale Modelling of Urban Climate. PhD thesis 4531, EPF Lausanne, Switzerland.

Richards PJ, Mallison GD, McMillan D, Li YF (2002) Pedestrian level wind speeds in downtown Auckland. palWind and Structures 5: 151-164

Riddle A, Carruthers D, Sharpe A, McHugh C, Stocker J (20049 Comparisons between FLUENT and ADMS for atmospheric dispersion modeling, Atmospheric Environment 38: 1029–1038

Robinson D, Haldi F, Kämpf J, Perez D (2011) Computer Modelling for Sustainable Urban Design, In: Computer Modelling for Sustainable Urban Design. Earthscan, London, Washington, DC, 2011, ISBN: 978-1-84407-679-6

Salim SM, Buccolieri R, Chan A, Di Sabatino S (2011a) Numerical simulation of atmospheric pollutant dispersion in an urban street canyon: Comparison between RANS and LES, J. of Wind Eng. and Industrial Aerodynamics 99: 103-113

Salim SM, Cheah SC, Chan A (2011b) Numerical simulation of dispersion in urban street canyons with avenue like tree plantings: Comparison between RANS and LES, Building and Environment 46: 1735-1746

Saneinejad S, Moonen P, Carmeliet J (2011) Analysis of convective heat and mass transfer at the vertical walls of a street canyon. J. of Wind Eng. & Industrial Aerodynamics 99: 424-433

Santamouris (Ed.) (2001) Energy and climate in the urban built environment. London: Earthscan

Santamouris (Ed.) (2006) Environmental Design Of Urban Buildings. Earthscan, London Washington DC, ISBN 190291642-5

Soulhac L, Garbero V, Salizzoni P, Mejean P, Perkins RJ (2009) Flow and dispersion in street intersections, Atmospheric Environment 43: 2981–2996

Stathopoulos T (2002) The numerical wind tunnel for industrial aerodynamics: real or virtual in the new millennium?, Wind and Structures 5: 193–208

Stathopoulos T, Lazure L, Saathoff P, Gupta A (2004) The effect of stack height, stack location and roof-top structures on air intake contamination - A laboratory and full-scale study. IRSST report R-392, Montreal, Canada

Strømann-Andersen J, Sattrup PA (2011) The urban canyon and building energy use: Urban density versus daylight and passive solar gains, Energy and Buildings 43: 2011-2020

Stupart AW (1989) A survey of literature relating to frost damage in bricks, Masonry International 3: 42-50

Tang W, Davidson CI (2004) Erosion of limestone building surfaces caused by wind-driven rain. 2. Numerical modeling, Atmospheric Environment 38:5601-5609

Tang W, Huber A, Bell B, Kuehlert K, Schwarz W (2005) Example application of CFD simulations for short-range atmospheric dispersion over the open fields of Project Prairie Grass, In: A&WMA Conference, Paper # 1243.

Tanimoto J, Hagishima A, Chimklai P (2004) An approach for coupled simulation of building thermal effect and urban climatology. Energy and Buildings 36: 781–793

Tominaga Y, Mochida A, Yoshie R, Kataoka H, Nozu T, Yoshikawa M, Shirasawa T (2008) AIJ guidelines for practical applications of CFD to pedestrian wind environment around buildings, J. of Wind Eng. and Industrial Aerodynamics, 96:1749-1761

Tominaga Y, Stathopoulos T (2010) Numerical simulation of dispersion around an isolated cubic building: model evaluation of RANS and LES, Building and Environment 45: 2231-2239

Tominaga Y, Stathopoulos T (2011) CFD modeling of pollution dispersion in a street canyon: Comparison between LES and RANS, J.l of Wind Eng. and Industrial Aerodynamics 99: 340-348

van Hooff T, Blocken B (2010) Coupled urban wind flow and indoor natural ventilation modelling on a high-resolution grid: A case study for the Amsterdam ArenA stadium, Environmental Modelling and Software 25: 51-65

van Hooff T, Blocken B, van Harten M (2011) 3D CFD simulations of wind flow and wind-driven rain shelter in sports stadia: influence of stadium geometry, Building and Environment 46: 22-3

Walton A, Cheng AYS (2002). Large-eddy simulation of pollution dispersion in an urban street canyon–Part II: idealised canyon simulation, Atmospheric Environment 36: 3615-3627

White RB (1967) The changing appearance of buildings, Her Majesty's Stationary Office, London, 64 p

Yoshie R, Mochida A, Tominaga Y, Kataoka H, Harimoto K, Nozu T, Shirasawa T (2007) Cooperative project for CFD prediction of pedestrian wind environment in the Architectural Institute of Japan. J. of Wind Eng. and Industrial Aerodynamics 95: 1551-1578

Yoshie R, Jiang G, Shirasawa T, Chung J (2011) CFD simulations of gas dispersion around high-rise building in non-isothermal boundary layer, Journal of Wind Engineering and Industrial Aerodynamics 99: 279-288